



## Spectroscopic characterization, thermogravimetric, DFT and biological studies of some transition metals complexes with mixed ligands of meloxicam and 1,10 phenanthroline



CrossMark

Sadeek A. Sadeek<sup>a\*</sup>, Amira A. Mohamed<sup>b</sup>, Wael A. Zordok<sup>a,c</sup>, Hanem M. Awad<sup>d</sup>, Sherif M. Abd El-Hamid<sup>e</sup>

<sup>a</sup> Department of Chemistry, Faculty of Science, Zagazig University, Zagazig, Egypt

<sup>b</sup> Department of Basic science, Zagazig Higher Institute of Engineering and Technology, Zagazig, Egypt

<sup>c</sup> Department of Chemistry, University College of Qanfuqda, Umm Al -Qura University, KSA

<sup>d</sup> Department Tanning Materials and Leather Technology, Centre of Excellence, National Research Centre, Cairo, Egypt

<sup>e</sup> Department of Basic Science, Higher Future Institute of Engineering and Technology, Mansoura, Egypt

### Abstract

A series of biologically active complexes were prepared using meloxicam (H<sub>2</sub>mel) and 1,10-phenanthroline monohydrate (Phen) as ligands. The compositions of all complexes were elucidated by infrared, electronic absorption and <sup>1</sup>H NMR spectroscopy, elemental analyses, magnetic moments, conductance and TG-DTG measurements. The analytical and spectroscopic data revealed that H<sub>2</sub>mel acts as a mono basic bidentate ligand binding through the oxygen of the amide and nitrogen of the thiazol groups, whereas Phen is coordinated through the two nitrogen atoms with slightly distorted octahedral geometry. The geometries of ligands and complexes were studied using density functional theory to predict properties of materials carried out using the hybrid density functional B3LYP level of theory. All studied complexes can be characterized as chemically soft with respect to the H<sub>2</sub>mel where  $\eta$  varied from 0.053 eV for Fe(III) complex to 0.089 eV for Zn(II) complex and  $\sigma$  varied from 11.236 to 18.868 eV, while  $\eta$  and  $\sigma$  for H<sub>2</sub>mel are 0.14 and 7.14 eV, respectively. The antibacterial activities of the ligands and metal complexes have been tested and the data showed that the complexes are significantly active against some bacterial species compared with H<sub>2</sub>mel.

*Keywords: Meloxicam; Phenanthroline; Spectra; Thermal analysis; antitumor activity; DFT*

### 1. Introduction

Metal chelation is implicated in several key biological processes where the coordination can occur between different metal ions and wide range of ligands [1, 2]. Complexes of mixed ligands have a strong role in biochemistry [2] because mixed chelation take place generally in biological fluids as millions of potential ligands contend for metal ions in vivo [3]. The oxamic class of drugs is extensively utilized in inflammatory and painful diseases of rheumatic and non- rheumatic origin. They are strong inhibitors of cyclooxygenase in vitro and in vivo by diminishing synthesis of prostaglandins, prostacyclin and thromboxane products [4]. From the coordination chemistry point of view, the oxicams are very interesting since they possess different heteroatoms able to coordinate metal ions. Interaction of oxicams with transition metals has been inspected by

conventional synthesis methods and various analytical methods [5]. Meloxicam ((H<sub>2</sub>mel) Scheme.1 (a)) is a derivative of the oxamic class of non-steroidal anti-inflammatory drug and has been specified as a selective COX-2 inhibitor with fewer adverse side effects [6]. It exhibits chemo preventive and chemo suppressive effects in special cancer lines [7], and is also used in treating osteoarthritis and rheumatoid diseases [8]. The oxicams as coordinative ligands have at least three distinctive coordination modes. In the H<sub>2</sub>mel complexes, the enol oxygen is deprotonated and remains uncoordinated to metal ions but instead is linked to the N-H group via a strong intramolecular hydrogen bond. The coordination of H<sub>2</sub>mel ligand is via the nitrogen atom of the thiazolyl ring and the amide oxygen atom [9]. This interaction results in the adoption of either the ZZZ-Hmel<sup>-</sup> or ZZE Hmel<sup>-</sup> conformation. In

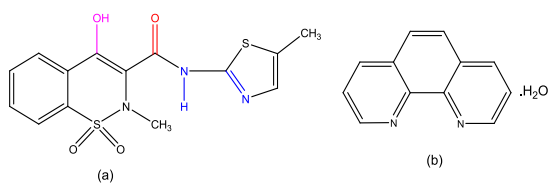
\*Corresponding author e-mail: [s\\_sadeek@zu.edu.eg](mailto:s_sadeek@zu.edu.eg); (Sadeek A. Sadeek).

Receive Date: 03 January 2021, Revise Date: 05 April 2021, Accept Date: 08 April 2021

DOI: 10.21608/EJCHEM.2021.56086.3211

©2021 National Information and Documentation Center (NIDOC)

comparison, 1,10-phenanthroline ((Phen) Scheme.1 (b)) is a hetero organic compound which acts as bidentate ligand chelating through the two nitrogen atoms. Metal complexes with phen and related ligands have been intensively investigated because of their numerous biological activities such as antitumor, antibacterial and antimicrobial properties [10]. This paper is in continuation of previous studies on metal - oximic complexes; here we report this synthesis and structural characterization of H<sub>2</sub>mel and Phen complexes with some of biologically relevant metal ions such as Fe(III), Co(II), Ni(II), Cu(II), Zn(II) and Zr(IV). The novel metal complexes prepared were characterized by infrared, ultraviolet visible, proton NMR spectroscopy, thermal analysis, melting point, magnetic susceptibility, elemental analyses and conductivity measurements. Density functional theory (DFT) was utilized to determine the optimized molecular geometry and energy gap  $\Delta E$ , absolute electronegativity,  $\chi$ , chemical potentials,  $P_i$ , absolute hardness,  $\eta$ , absolute softness,  $\sigma$ , global electrophilicity,  $\omega$ , global softness,  $S$ , and additional electronic charge,  $\Delta N_{max}$ . Also, the antibacterial activities and cytotoxicity of the compounds have been examined.



**Scheme 1** (a) H<sub>2</sub>mel (4-hydroxy-2-methyl-N-(5-methyl-2-thiazoyl)-2H-1,2-benzothiazine-3-carboxamide-1,1-dioxide). (b) 1,10-phenanthroline monohydrate (Phen).

## 2. Experimental

### 2.1. General considerations

All reagents and solvents were analysed and utilized without further purification. Meloxicam was a gift from Amoun Pharmaceutical Company. Analytical grade 1,10-phenanthroline, KOH, ethanol, FeCl<sub>3</sub> (anhydrous), CoCl<sub>2</sub>.6H<sub>2</sub>O, Ni(CH<sub>3</sub>COO)<sub>2</sub>.2H<sub>2</sub>O, CuCl<sub>2</sub>.2H<sub>2</sub>O, ZnCl<sub>2</sub>.H<sub>2</sub>O and ZrOCl<sub>2</sub>.8H<sub>2</sub>O were commercial products (from Aldrich and Fluka Chemical Company). The elemental analysis was accomplished by a CHNS elemental analyzer titled Perkin Elmer 2400 series. The percent of the metal ions were identified gravimetrically by conversion the solid products into metal or metal oxide and also identified by using atomic absorption method. Spectrometer model PYE-UNICAM SP 1900 supplied with the corresponding lamp was used for this work. Fourier transform-IR spectra in KBr discs were measured in the range from

4000-400 cm<sup>-1</sup> with a Fourier Transform-IR 460 PLUS Spectrophotometer. Proton NMR spectra were recorded on a Varian Mercury VX-300 NMR Spectrometer using Dimethyl sulfoxide-d<sub>6</sub> as solvent. TG-DTG measurements were done under N<sub>2</sub> atmosphere within the temperature range from room temperature to 1000 °C using TGA-50H Shimadzu, the mass of sample was accurately weighted out in an aluminum crucible. Electronic absorption spectra were measured on an UltraViolet-3101PC Shimadzu spectrophotometer. The absorption spectra were recorded as solutions in DMSO. Magnetic susceptibilities of the samples were done on a Sherwood scientific magnetic balance using Gouy balance at room temperature using Mercury(II) Tetrathiocyanatocobaltate(II) as calibrant. The molar conductance of 1×10<sup>-3</sup> M solutions of the ligands and their complexes in dimethylformamide was measured at room temperature using CONSORT K410. Melting points were recorded on a Buchi apparatus.

### 2.2. Synthesis of mixed ligand metal complexes

The black solid complex [Fe(Hmel)(Phen)(H<sub>2</sub>O)<sub>2</sub>]Cl<sub>2</sub> (A) was prepared by mixing 1 mmol (0.351 g) of (H<sub>2</sub>mel) with 1mmol (0.055g) of KOH in 40 ml absolute ethanol and 1mmol (0.198 g) of (Phen) with the same ratio 1 mmol (0.1622 g) of iron(III) chloride. The mixture was refluxed for 3 h. The black precipitate was filtered off and dried under vacuum over anhydrous CaCl<sub>2</sub>. The orange, pale green, dark green, pale yellow and yellowish solid complexes of [Co(Hmel)(Phen)(H<sub>2</sub>O)<sub>2</sub>]Cl<sub>2</sub>.2H<sub>2</sub>O (B), [Ni(Hmel)(Phen)(H<sub>2</sub>O)<sub>2</sub>](CH<sub>3</sub>COO).1.5H<sub>2</sub>O (C), [Cu(Hmel)(Phen)(H<sub>2</sub>O)<sub>2</sub>]Cl<sub>2</sub>.2H<sub>2</sub>O (D), [Zn(Hmel)(Phen)(H<sub>2</sub>O)<sub>2</sub>]Cl (E) and [ZrO(Hmel)(Phen)]Cl<sub>2</sub>.3H<sub>2</sub>O (F) were prepared in a similar manner described above by using CoCl<sub>2</sub>.6H<sub>2</sub>O, Ni(CH<sub>3</sub>COO)<sub>2</sub>.2H<sub>2</sub>O, CuCl<sub>2</sub>.2H<sub>2</sub>O, ZnCl<sub>2</sub>.H<sub>2</sub>O and ZrOCl<sub>2</sub>.8H<sub>2</sub>O, respectively, in ethanol as a solvent with 1:1:1:1 (M<sup>n+</sup>:H<sub>2</sub>mel:KOH:Phen) molar ratio.

### 2.3. Antimicrobial Investigation

Antimicrobial activity of compounds was investigated by modified method of Beecher and Wong [11] against different bacteria and fungi species, such as Escherichia Coli ATCC11229, Coliform ATCC8729, Staphylococcus aureus ATCC6538, Salmonella typhi ATCC14028, Citrobacter, Listeria and Aspergillus niger. The tested microorganisms were isolated from Egyptian soil and water then identified. The nutrient agar medium for antibacterial was (0.5% Peptone, 0.1% Beef extract, 0.2% Yeast extract, 0.5% NaCl and 1.5% Agar-Agar) and Czapeks Dox medium for antifungal (3%) Sucrose, 0.3% NaNO<sub>3</sub>, 0.1%

$K_2HPO_4$ , 0.05% KCl, 0.001%  $FeSO_4$ , 2% (Agar-Agar) was prepared [12] then cooled to 47 °C and seeded with tested microorganisms. Sterile water agar layer was poured then solidified, the prepared growth medium for fungi and bacteria (plate of 12 cm diameter, 15 ml medium plate). After solidification 5 mm diameter holes were holed by a sterile cork-borer. The examined compounds, i.e., ligands and their complexes, were introduced in petri-dishes (only 0.1 ml) after dissolving in DMF at  $1.0 \times 10^{-3}$  M. These culture plates were then incubated at 37 °C for 20 h for bacteria and for seven days at 30 °C for fungi. The activity was estimated by measuring the diameter of the inhibition zone (in mm). Microbial growth inhibition was calculated with reference to the positive control, ( $H_2mel$ ).

#### 2.4. In-vitro cytotoxic activity

Cell culture of HCT-116 (human colorectal carcinoma), HepG2 (human hepatocellular carcinoma) and MCF-7 (human breast adenocarcinoma) cell lines were bought from the American Type Culture Collection (Rockville, MD) and preserved in DMEM medium which was accomplished with 10% heat-deactivated FBS (fetal bovine serum), 100U/ml penicillin and 100U/ml streptomycin. The cells were matured at 37 °C in a moisten atmosphere of 5%  $CO_2$ .

**MTT cytotoxicity assay:** The cytotoxicity activity against MCF-7, HepG2 and HCT-116 human cancer cell lines was estimated using the 3-[4,5-dimethyl-2-thiazolyl]-2,5-diphenyl-2H-tetrazolium bromide (MTT) assay, which is based on the cleavage of the tetrazolium salt by mitochondrial dehydrogenases in viable cells [13]. Cells were dispensed in a 96 well sterile microplate ( $5 \times 10^4$  cells/well), and incubated at 37 °C with series of different concentrations, in DMSO, of each tested compound or Doxorubicin (positive control) for 48 h in a serum free medium prior to the MTT assay. After incubation, media were carefully isolated, 40  $\mu$ L of MTT (2.5 mg/mL) were added to each well and then incubated for an additional 4 h. The purple formazan dye crystals were solubilized by the addition of 200  $\mu$ L of DMSO. The absorbance was measured at 590 nm using a Spectra Max Paradigm Multi-Mode micro plate reader. The relative cell viability was detailed as the mean % of viable cells in comparison with the untreated control cells. All experiments were managed in triplicate and reduplicated on three different days. All the values were represented as mean  $\pm$  SD.  $IC_{50}$  values were determined by probit analysis by SPSS Incprobit analysis (IBM Corp., Armonk, NY, USA).

### 3. Results and Discussion

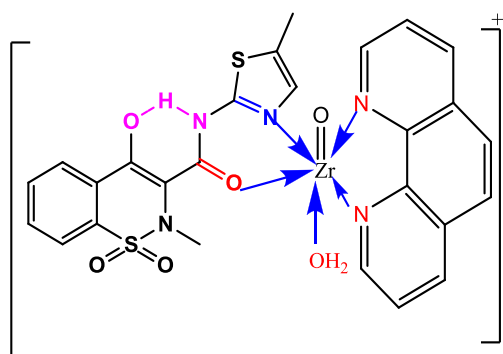
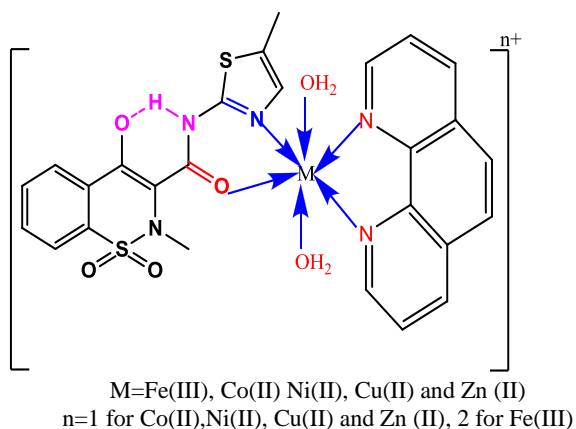
Elemental analysis and physical characteristics of compounds are reported in Table 1. The analytical results demonstrate that all the prepared complexes have 1:1:1 (M:  $H_2mel$ : Phen) stoichiometry. The molar conductance measurements in DMF of all complexes at room temperature are in the range from 78.15- 139.12  $S\ cm^2\ mol^{-1}$ , these values are expected for an electrolyte complex [14]. Qualitative reactions detected the presence of  $Cl^-$  and  $CH_3COO^-$  ions as counter ions. The magnetic moments (as B.M.) of the complexes were measured at room temperature and point out the complexes are paramagnetic nature with molecular geometries octahedral except the Zr(IV) and Zn(II) complexes which were found to be diamagnetic. The solid complexes are soluble in dimethyl sulfoxide and dimethylformamide. The structures and properties were characterized by Fourier-transform-IR, Ultraviolet-Vis., proton NMR spectroscopy as well as thermal analysis.

#### 3.1. IR absorption spectra

The IR spectroscopy has proven to be the most useful technique in this study to give accurate information to deduce the mode of bonding of the ligands to the metal ions. The fundamental bands occurring in the infrared spectra of the free ligands and their complexes have been compared to confirm the bonding sites in the chelating ligands. The  $H_2mel$  shows the following observed bands at 3438, 3289, 1620, 1550, 1346 and 1183  $cm^{-1}$  which have been attributed to the stretching vibration of  $\nu(O-H)_{enolate}$ ,  $\nu(N-H)_{amide}$ ,  $\nu(C=O)_{amide}$ ,  $\nu(C=N)_{thiazoyl}$ ,  $\nu(SO_2)_{asym}$  and  $\nu(SO_2)_{sym}$ , respectively [14, 15]. The absence of absorption bands in the region 3289-3200  $cm^{-1}$  in the spectra of complexes indicates that the N-H group of the  $Hmel^-$  is involved in a strong intra molecular hydrogen bond to the enolate oxygen. The stretching vibrations for the amide C=O group circa 1620  $cm^{-1}$  and C=N for thiazoyl ring around 1550  $cm^{-1}$  in the free ligand shifted to the lower wavenumber in the complexes which indicate the coordination of the  $Hmel^-$  anion through these two groups. The band due to the vibrational  $\nu(C=N)$  mode at 1586  $cm^{-1}$  in Phen was observed to be shifted to lower frequency, at 1538-1600  $cm^{-1}$  in the metal complexes indicating the involvement of the pyridine ring nitrogen in complex formation [16]. This is further confirmed by the appearance of new absorption bands in the range 685-467  $cm^{-1}$  due to  $\nu(M-O)$  and  $\nu(M-N)$  bands which are not observed in the spectrum of the free ligands. The slight shift of bands due to the  $SO_2$  group ( $\nu_{as}$  and  $\nu_s$ ) to lower frequency may be linked to hydrogen bonding effects [17], or electronic density changes on the sulfur.

**TABLE 1. Elemental analysis and physico-analytical data for H<sub>2</sub>mel, Phen and their metal complexes.**

Compounds F.Wt. (M.F.)	Yield, %	Mp, °C	Color	Found (Calcd.) (%)					$\mu_{\text{eff}}$ , B M	$\Lambda$ , S cm <sup>2</sup> mol <sup>-1</sup>
				C	H	N	M	Cl		
(H <sub>2</sub> mel) 351.39 (C <sub>14</sub> H <sub>13</sub> N <sub>3</sub> O <sub>4</sub> S <sub>2</sub> )	-	254	Yellow	74.79 (74.82)	3.69 (3.72)	11.94 (11.97)	-	-	-	13
Phen 198.20 (C <sub>12</sub> H <sub>10</sub> N <sub>2</sub> O)	-	100	White	72.68 (72.72)	5.06 (5.09)	14.10 (14.13)	-	-	-	5.20
A 693.45 (FeC <sub>26</sub> H <sub>24</sub> N <sub>5</sub> O <sub>6</sub> S <sub>2</sub> Cl <sub>2</sub> )	88.5	240	Black	44.93 (44.96)	3.44 (3.48)	10.02 (10.06)	8.00 (8.02)	10.18 (10.21)	1.80	139.1
B 697.04 (CoC <sub>26</sub> H <sub>28</sub> N <sub>5</sub> O <sub>8</sub> S <sub>2</sub> Cl)	80.2	280	Orange	44.70 (44.74)	3.96 (3.99)	10.00 (10.02)	8.37 (8.40)	5.02 (5.06)	1.60	87.5
C 711.29 (NiC <sub>28</sub> H <sub>30</sub> N <sub>5</sub> O <sub>9.5</sub> S <sub>2</sub> )	84.3	254	Pale green	47.22 (47.20)	4.17 (4.20)	9.77 (9.81)	8.18 (8.22)	-	3.31	78.2
D 701.65 (CuC <sub>26</sub> H <sub>28</sub> N <sub>5</sub> O <sub>8</sub> S <sub>2</sub> Cl)	82.5	210	Dark green	44.41 (44.44)	3.93 (3.97)	9.92 (9.96)	9.00 (9.02)	5.00 (5.03)	1.70	82.7
E 667.49 (ZnC <sub>26</sub> H <sub>24</sub> N <sub>5</sub> O <sub>6</sub> S <sub>2</sub> Cl)	75.0	266	Pale yellow	46.68 (46.71)	3.52 (3.55)	10.45 (10.46)	9.74 (9.77)	5.25 (5.29)	Dia- magnetic	88.3
F 745.33 (ZrC <sub>26</sub> H <sub>28</sub> N <sub>5</sub> O <sub>9</sub> S <sub>2</sub> Cl)	87.2	220	Yellow	41.80 (41.84)	3.69 (3.72)	9.40 (9.44)	12.17 (12.20)	4.70 (4.73)	Dia- magnetic	87.4

**Scheme 2** The chelation mode of Fe(III), Co(II), Ni(II), Cu(II), Zn (II) and Zr(IV) with Hmel and Phen.**3.2. UV-Visible spectra**

The electronic absorption spectra supply credible information about the ligand configuration in transition metal complexes. The electronic absorption spectra of H<sub>2</sub>mel and Phen along with (A), (B), (C), (D), (E) and (F) complexes in the wavelength from 200 to 800 nm range in DMSO were recorded. The data indicated that H<sub>2</sub>mel absorbed at 266 and 362 nm which may be assigned to  $\pi-\pi^*$  and  $n-\pi^*$  transitions, respectively. The electronic absorption spectrum of Phen shows bands at 273 and 350 nm which may be assigned to  $\pi-\pi^*$  and  $n-\pi^*$  transitions, respectively [15, 18]. The absorption spectra for (A), (B), (C), (D), (E) and (F) complexes were practically identical with that of free ligands, some shifted of the bands to lower or higher values were observed which indicative of chelation through the donor atoms of the ligands. Also, the complexes showed new bands in the range 530-578 nm, which may be assigned to ligand-metal charge transfer [19]. The electronic spectrum of (A) complex displays absorption band at 610 nm may assigned to spin forbidden  ${}^6A_1 \rightarrow {}^4T_2$  ( ${}^4G$ ) transition [20]. For (B) complex shows absorption band at 625 nm which may be assigned to  ${}^6T_{1g}(F) \rightarrow {}^4T_{1g}(P)$  transition suggesting that there is an octahedral geometry around Co(II) [21]. The (C) complex shows absorption band at 614 nm which may be assigned to  ${}^3A_{2g} \rightarrow {}^3T_{1g}(P)$  transition and supporting distorted octahedral geometry [21]. The bands observed at 604 nm for (D) complex may be assigned to  ${}^2B_{1g} \rightarrow {}^2E_g$  transition

[22]. Also, the value of the experimentally magnetic moment determined in (D) complex (1.70 B.M.) closely approximates the spin value (1.73 B.M.) expected which is further evidence for an octahedral geometry. The (C) complex with magnetic moment value of 3.31 B.M. which is in normal range reported for octahedral Ni(II) complexes ( $\mu = 2.9 - 3.3$  B.M) [23].

### 3.3. $^1\text{H}$ NMR spectra

The  $^1\text{H}$  NMR spectra of compounds were recorded in deuterated dimethyl sulfoxide at room temperature. Some new bands observed in the complexes in the range present 3.08-3.46 ppm may be indicated to water molecules of coordinated and adsorbed in the surface of metal complexes [24]. The signals at 7.49-7.80 ppm and 7.26-8.81 ppm (m, Ar-H) assigned to aromatic protons observed in  $\text{H}_2\text{mel}$  and Phen ligands show shifts in the complexes (7.45-8.14 ppm). This shift is due to variation in electron density upon chelation [25]. The singlet at 14.50 ppm due to the proton of OH enolate group observed in the spectrum of the free  $\text{H}_2\text{mel}$  is not observed in the spectra of (A)-(F) complexes due to the strong intra molecular hydrogen bond to the enolate oxygen. This is in consistent with the data previously reported from the infrared spectrum [15]. Peaks of free  $\text{H}_2\text{mel}$  were present in spectra of the complexes with shifted to lower or higher upon coordination with the metal.  $^1\text{H}$  NMR spectral studies of paramagnetic Fe(III), Mn(II), Co(II), Ni(II), and Cu(II) complexes have been reported in the literature [15, 26].

### 3.4. Thermal analysis studies

Thermal analysis was used as a probe to give evidence for the associated water or solvent molecules in the coordination sphere or in the crystalline network. Thermal studies have been achieved using a thermo gravimetric (TG) technique. The thermal analyses of  $\text{H}_2\text{mel}$  and Phen have previously been reported in the literature [15]. The TG curve of  $\text{H}_2\text{mel}$  at a maximum temperature 265 °C with 93% weight loss assigned to the loss of  $6\text{C}_2\text{H}_2 + 2\text{SO}_2 + 1.5\text{N}_2 + 0.5\text{H}_2$  [15]. The thermal degradation of Phen takes place in two degradation stages. The first stage occurs at 95 °C maximum and is accompanied by a weight loss of 8.02%. The second decomposition stage occurs at maximum 278 °C with a weight loss of 91.98% corresponding to loss of  $5\text{C}_2\text{H}_2 + \text{C}_2\text{N}_2$  [27]. Thermal decomposition of (A) and (E) complexes were done in two main steps. The first step occurs at one maximum temperature 259 °C for (A) complex and at 270 °C for (E) complex with a weight loss of 31.00% and 32.01% for (A) and (E) complexes, respectively, corresponding to the loss of  $6\text{C}_2\text{H}_2 + 2\text{NO}$  molecules. The decomposition mechanisms are only based on speculation and the thermal analysis without a complementary technique (gas chromatography). The

second step at 414 °C for A complex and 348 °C for (E) complex and a weight loss of 59.21% and 55.40% corresponding to the loss of  $\text{Hmel}^+$  ion giving Fe+C and ZnO as final products. Thermal decomposition of complex (B) proceeds in three stages. The loss of the hydrated water molecules takes place in the temperature range 35–100 °C, with a weight loss 5.15%, (calc. 5.16%) corresponding to  $2\text{H}_2\text{O}$ . The second temperature range 190–289 °C corresponding to loss of two coordination water and Phen molecules (found 31.00%, calc. 31.02%). The final stage is showing the decomposition of  $\text{Hmel}^+$  ion giving  $\text{CoO} + 10\text{C}$  as residue. The TG of (C), (D) and (F) complexes proceeds with three main steps. The first stage occurs at 127, 66 and 62 °C maxima with a weight loss 3.73%, 5.18% and 7.25% corresponding to the loss of  $1.5\text{H}_2\text{O}$ ,  $2\text{H}_2\text{O}$  and  $3\text{H}_2\text{O}$ . The complexes were dried under vacuum over anhydrous  $\text{CaCl}_2$ . The second step occurs at 198 and 289 °C for C complex, at 226 and 276 °C for (D) complex and at 318 °C for (F) complex maxima with weight loss 30.38%, 30.60% and 26.76% corresponding to the loss of coordinated water and Phen. The final step found at 378, 449 and 817 °C for (C) complex, at 805 °C for (D) complex and 826 °C for (F) complex with weight loss 43.89%, 45.85% and 46.97% corresponding to the loss of  $\text{Hmel}^+$  ion giving  $\text{NiO} + 7\text{C}$ ,  $\text{CuO} + 4\text{C}$  and  $\text{ZrO}_2 + 2\text{C}$  as a final products.

### 3.5. Antimicrobial efficiency and determination of MIC for the compounds

The main aim of the production and synthesis of any antimicrobial compound is to inhibit the causal microbe without any side effects on the patients. In measuring the antibacterial activity of the compounds under study we used more than one tested organism to raise the chance of detecting antibiotic principles in the compounds. Being evaluated, the antibacterial activity of the  $\text{H}_2\text{mel}$ , Phen and their metal complexes against different bacteria and fungi species, such as *Escherichia Coli* ATCC11229, *Coliform* ATCC8729, *Staphylococcus aureus* ATCC6538, *Salmonella typhi* ATCC14028, *Citrobacter*, *Listeria* and *Aspergillus niger* were tested and compared with Amoxycillin/ Clavulanic and Cetaxime (Antibacterial agents). The data showed that the complexes (A), (B), (D) and (F) showed very highly significant against *S. aureus* and (A) complex showed a highly significant against *Listeria* and *S. typhi* ATCC14028. The two complexes (B) and (E) showed a highly significant against coliform. While (C) complex showed no significant against all bacteria screened in this study. The results made certain that (A) complex is more efficient than all other complexes. The tested compounds were found to exhibit no antifungal action. The high sensitivity of the complexes have been assigned to hyper-conjugation of the coordinated aromatic Lewis bases, which elevates the

net electron density on the coordinated metal ion and consequently higher antimicrobial activity [28]. In general, metal complexes are more efficient than the ligand because metal complexes may carry out as a vehicle for activation of ligands as the principle cytotoxic species [29]. The antimicrobial activities of H<sub>2</sub>mel, Phen and their complexes were determined by minimum inhibitory concentration (MIC; μg) studies. The data showed that the (F) complex has the lowest MIC for *S. aureus* (14.88 μg) followed by (A), (B) and (D) complexes. For Coliform, the lowest minimum inhibition concentration appeared for (B) complex followed by (E) complex.

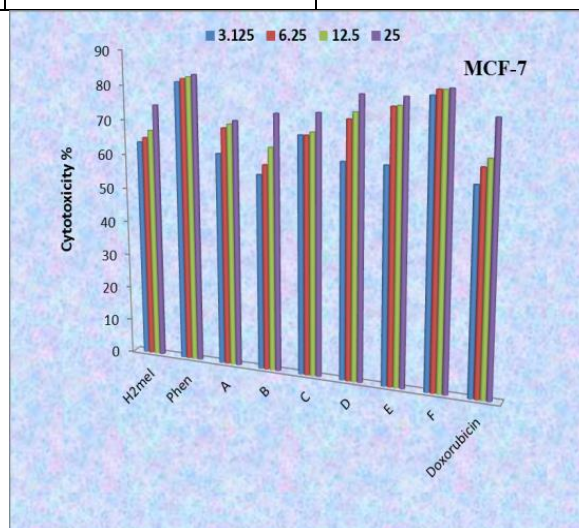
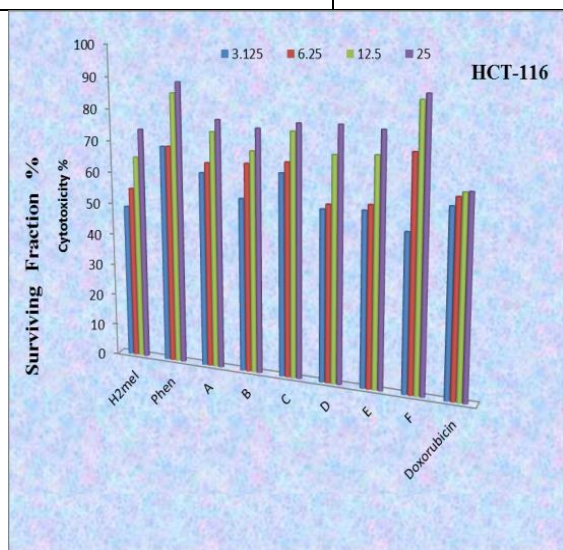
### 3.6. Cytotoxicity screening

The ligands and their complexes were assessed in vitro for their action against HCT-116, HepG2 and MCF-7 human cancer cells. The percentages of intact cells were measured and compared to those of the control. Activities of these compounds against the three carcinoma cell lines were compared to the activity of doxorubicin as the

standard. All compounds repressed the three cancer cells in a dose-dependent way (Fig. 1). In case of HCT-116 human cancer cells, Table 2 show that, seven compounds (Phen), (F), (C), (A), (B), (E) and (D), respectively were more potent cytotoxic compounds; only one compound (H<sub>2</sub>mel) had was slightly less active compared to doxorubicin. In case of MCF-7 human breast cancer cells, seven compounds (F), Phen, H<sub>2</sub>mel, (E), (D), (C) and (A), respectively were more potent cytotoxic compounds; one compound (B) was slightly less active compared to doxorubicin against MCF-7 cancer cells. In case of HepG2 human liver carcinoma cells, five compounds (F), H<sub>2</sub>mel, (D), (E) and Phen were more potent than the reference drug; the rest of the compounds (B), (C) and (A), respectively were slightly less active against HepG2 compared to doxorubicin (Table 2). From the above mentioned results, one can deduce that all the eight synthesized compounds are strong anticancer drug candidates.

**TABLE 2.** IC<sub>50</sub> of the synthesized compounds against the three cancer cell lines according to the MTT assay.

Compounds	IC <sub>50</sub> (μM) ± SD		
	HCT-116	MCF-7	HepG2
H <sub>2</sub> mel	10.3 ± 3.5	1.5 ± 0.5	9.3 ± 3.2
Phen	0.6 ± 0.3	0.5 ± 0.2	9.8 ± 3.5
A	5.2 ± 1.7	6.3 ± 2.5	11.7 ± 4.2
B	6.8 ± 2.1	8.5 ± 3.4	10.8 ± 3.3
C	4.1 ± 2.1	4.9 ± 2.0	11.2 ± 5.1
D	7.6 ± 2.1	3.8 ± 1.9	9.5 ± 3.9
E	7.3 ± 2.3	2.9 ± 1.2	9.6 ± 3.1
F	1.8 ± 0.6	0.2 ± 0.2	6.4 ± 2.5
Doxorubicin	9.4 ± 3.9	6.7 ± 2.9	10.4 ± 3.6



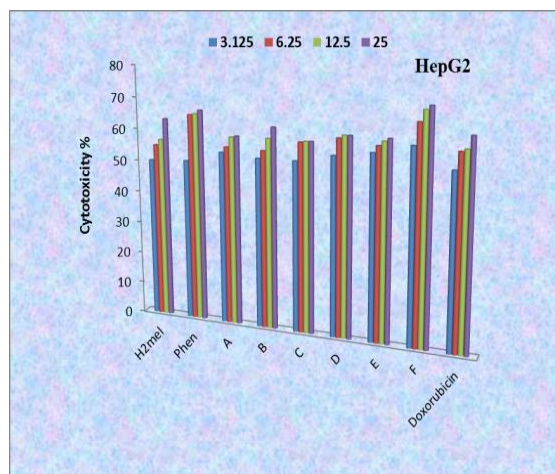


**Fig. 1** Dose dependent cytotoxic activities of the synthesized compounds against HCT-116, MCF-7 and HepG2 cancer cells according to the MTT assay.

#### 4. Computational studies

The geometric parameters (dipole moment, dihedral angles, bond angle and bond length) and energies at a highly accurate for H<sub>2</sub>mel, (A), (B), (C), (D), (E) and (F) compounds were computed by DFT calculations at the B3LYP/CEP-31G level of the theory, using the GAUSSIAN 98W package of the programs [30] along with the B3LYP functional and Lee Yang Parr's correlation functional. In addition, the B3LYP/CEP-31G level of theory [31] basis set was applied for all calculations. The atomic charges were computed using the natural atomic orbital populations. The high basis set was chosen to detect the energies at a highly accurate level.

##### 4.1. Geometrical structure of H<sub>2</sub>mel

The structure of H<sub>2</sub>mel with atomic numbering figure is shown in Fig. 2. The calculated bond lengths and dihedral angles were listed in Table 3. The data assured that the exact single O–H length formed with bond length 1.03 Å [32], which excludes the formation of hydrogen bonding [33]. The value of the dihedral angles proved that the two donating atoms O17 and N19 are lying in two opposite directions (trans form) in the same plane and C1=O17 of the –CONH group is lying in the same plane of the thiazole ring and lying in the same direction of S20 of thiazole ring. According to all values of the dihedral angles, the H<sub>2</sub>mel is completely sp and can't act as bidentate ligand to a metal ion through O17 of the –CONH group and N19 of the thiazole group without rotation of thiazole group around N2–C18 bond because the nitrogen atom N19 of thiazole ring is lying in trans position respect to the oxygen atom O17 of –CONH group. The pronounced steric effects existing within the molecule create planar structure with a dihedral angle C18N2C1V3 -179.91° between the two units of molecule; substituted thiazol ring residue and benzothiazine ring and makes the planer molecule quite labile and major changes occur in the

configuration of the H<sub>2</sub>mel in presence of metal ions [34]. In the optimized geometry of H<sub>2</sub>mel the calculated dihedral angles H30N2C1O17, (-177.63° ≈ 180.0°) and H30N2C18N19, (-10.29° ≈ 0 0°) confirming that a Trans configuration of H30, O17 and cis sites for N19, H30 atoms. The values of the dihedral angles; O17C1C3C5, (-153.59°) and N2C1C3N4 (-143.52°) means that benzothiazene ring is slightly deviated from the plane of amide group with a small rotation about the C1–C3 bond. The above rotation in case of chelation for H<sub>2</sub>mel with metal ions inhibits hydrogen bonding between H30 and O16 as suggested before [35]. The charge distribution on H<sub>2</sub>mel is slightly weak dipole, μ = 8.57 D refers to the absence of a net positive pole and a net negative pole on the molecule. The computed data given in Table 3 are compatible with those obtained from X-ray data [35]. All theoretical calculations were carried out in gas phase to predict the exact structure of all studied compounds and show the relation between atoms involved in each compound or complex. Also study the degree of stability of the ligand and its complexes from the point view of the value of total energy, dipole moment and charge density over all atoms. The structure was confirmed by the electronic excitation.

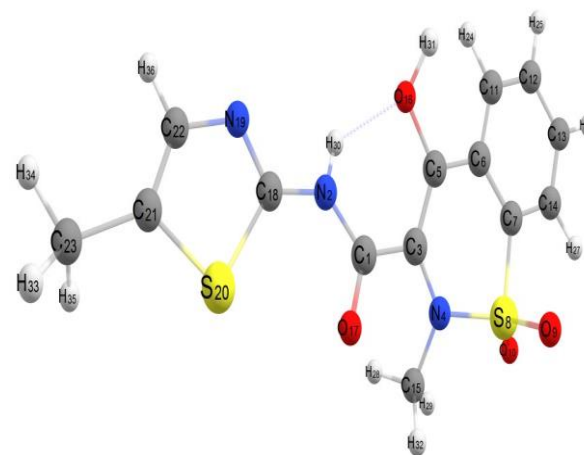


**Fig. 2** DFT-Optimized geometry of H<sub>2</sub>mel.

##### 4.2. Geometrical structure of complexes

The complexes consist of one unit from H<sub>2</sub>mel and Phen beside two water molecules to complete the octahedral structure of metal ion. The bond lengths and angles of complexes are reported in supplementary material. According to experimental data the complexes are six coordinated with a regular octahedral environment around the metal ion. According to computational data, the equatorial plane in all complexes is occupied by four donating atoms, two donating atoms of Hmel<sup>-</sup> ion (O5 and N1), Phen (N6 and N9) and two water molecules (O10 and O11), while the axial plane is occupied by (N1) of Hmel<sup>-</sup> ion and O10) of H<sub>2</sub>O. The angles of

N1-M-O10 and O10-M-O11 are 172.05° and 86.52°, respectively, which indicate that Hmel<sup>-</sup> ion and Phen not lying in the same plane but they are perpendicular to each other and two water molecules are lying in cis form. Also, the angles around the M with surrounding oxygen atoms vary from 78.52° to 176.55°, these values agree with these expected for a slightly regular octahedron. The bond length of C=O (C4-O5) in all metal complexes varied from (1.357-

1.359 Å) is longer than that in the free ligand (1.255 Å). This variation confirms the coordination via amide C=O group and C=N for thiazoyl ring [36]. The total energy, heat of formation and dipole moment of all complexes are reported in supplementary material.

**TABLE 3. Equilibrium geometric parameters bond lengths (Å), bond angles (°), dihedral angles (°), total energy (eV), heat of formation (k cal/mol) and dipole moment of the meloxicam ligand by using DFT calculations.**

Bond length (Å)			
C7-S8	1.737	S8-O10	1.439
C1-C3	1.371	O16-H31	1.021
C1-O17	1.255	C3-N4	1.354
C1-N2	1.378	C5-O16	1.364
C3-C5	1.354	N19-C18	1.353
N4-S8	1.633	N2-H30	1.017
N4-C15	1.458	C22-N19	1.359
C18-N2	1.342	C18-S20	1.819
C21-S20	1.812	O16.....H30	1.933
S8-O9	1.439		
Bond angle (°)			
C1C3C5	118.65	N2C1O17	121.03
C1C3N4	120.15	C15N4S8	113.95
C1N2C18	125.12	N2C18S20	128.65
N2C18N19	121.59	C3C1O17	118.80
N2C1C3	119.94	C3C5O16	118.55
C6C5O16	118.88	O9S8O10	125.41
Dihedral angles (°)			
O16C5C3N4	175.29	C1N2C18S20	-8.86
O16C5C3C1	0.34	N2C1C3N4	-143.52
N19C18N2C1	166.87	C22N19C18N2	-179.99
C18N2C1C3	-179.91	N2C1C3C5	31.48
C5C3C1O17	-153.89	C18N2C1O17	5.59
C11C6C5O16	-7.71	O17C1C3N4	31.11
Total energy/ eV		-219.42	
Heat of formation k cal/mol		-6620.33	
Total dipole moment/D		8.57	

#### 4.3. Charge distribution analysis

The charge distribution analysis on the optimized geometry arrangement of the compounds was carried out on the basis of normal population analysis (NPA) and data are adduced in Table 4. The data given in Table 4 showed a relatively high charge density on (D) and (F) complexes (0.351 and 0.365 eV) compared with the other complexes. Also, the charge distribution on Hmel<sup>-</sup> ion points out the absence of a negative and positive pole on the molecule, as a result the molecule has a weak calculated dipole, in the gas phase  $\mu = 8.57$  D. The negative charge is delocalized on oxygen and nitrogen, while all the hydrogen atoms in the complexes carry positive charge. The carbons directly attached to nitrogen and oxygen atoms, (C2, C4, C7 and C9) have more positive values due to electronegative character of oxygen and nitrogen atoms. The charge density for our complexes varies from 0.365 to 0.025 eV which indicate an electron

back-donation from the metal ions to the  $\pi^*$  sp orbital's of the Hmel<sup>-</sup> ion. This conclusion is further confirmed by comparing the values of the calculated charge density on the donating atoms in Hmel<sup>-</sup> ion and complexes. All calculations were carried out by using same basis set, the B3LYP/CEP-31G level of theory [31] basis set was applied for the all calculations.

#### 4.4. Molecular Orbitals and Frontier

The energy gap ( $\Delta E$ ) between HOMO and LUMO levels of our compounds were calculated and varied from 0.106 eV for (A) complex and 0.28 eV for H<sub>2</sub>mel (Table 4). The value of  $\Delta E$  is correlating with the reactivity and stability of the executed molecule and showed the nature of the molecule. The data showed all studied complexes have lower  $\Delta E$  than H<sub>2</sub>mel, so these complexes more reactive and termed chemically soft molecules.

**Excited state:** The TD-DFT at the B3LYP level proved to give accurate description of the ultraviolet visible spectra by using G03W program [37]. Time-dependent density functional response theory (TD-DFT) has been lately reformulated [38] to count separate transition energies and wavered strengths and has been applied to a number of

different atoms and molecules [39]. Bauernschmitt and Ahlrichs included hybrid functional suggested in the counting of the excitation energies. These hybrid methods typically comprise a considerable improvement over conventional Hartree-Fock (HF) based methods [40].

**TABLE 4.** Calculated charges on donating sites and energy values (HOMO, LUMO, Energy gap  $\Delta E/eV$ , hardness ( $\eta$ ), global softness (S), electro negativity ( $\chi$ ), absolute softness ( $\sigma$ ), chemical potential (Pi), global electrophilicity ( $\omega$ ) and additional electronic charge ( $\Delta N_{max}$ ) of the free ligand meloxicam and studied complexes by using DFT calculations. (( I ) is ionization energy, ( A ) is an electron affinity)

Parameters	H <sub>2</sub> mel	(A)	(B)	(C)	(D)	(E)	(F)
M	-	0.099	0.046	0.025	0.351	0.092	0.365
N <sub>thiazole</sub>	-0.318	-0.142	-0.158	-0.184	-0.101	-0.157	-0.156
O <sub>carbimide</sub>	-0.592	-0.418	-0.451	-0.425	-0.185	-0.455	-0.376
N <sub>6phen</sub>	-	-0.116	-0.119	-0.096	-0.069	-0.102	-0.072
N <sub>9phen</sub>	-	-0.098	-0.088	-0.067	-0.065	-0.091	-0.061
HOMO, H	-0.384	-0.338	-0.352	-0.356	-0.327	-0.369	-0.371
LUMO, L	-0.104	-0.232	-0.235	-0.234	-0.193	-0.192	-0.201
I = -H	0.384	0.338	0.352	0.356	0.327	0.369	0.371
A = -L	0.104	0.232	0.235	0.234	0.193	0.192	0.201
$\Delta E = L-H$	0.28	0.106	0.117	0.122	0.134	0.177	0.170
$\eta = (I-A)/2$	0.14	0.053	0.059	0.061	0.067	0.089	0.085
$\chi = -(H+L)/2$	0.244	0.285	0.294	0.295	0.260	0.281	0.286
$\sigma = 1/\eta$	7.14	18.868	16.949	16.393	14.925	11.236	11.765
$S = 1/2 \eta$	3.57	9.434	8.475	8.197	7.463	5.618	5.882
Pi = - $\chi$	-0.244	-0.285	-0.294	-0.295	-0.260	-0.281	-0.286
$\omega = (Pi)^2/2 \eta$	0.213	0.766	0.733	0.713	0.504	0.487	0.481
$\Delta N_{max} = \chi/\eta$	1.74	5.377	4.983	4.836	3.881	3.157	3.365

## Conclusion

In conclusion, innovative mixed ligand complexes were successfully prepared. The data obtained from the analytical and physicochemical analyses confirmed the stability of the new compounds. <sup>1</sup>H NMR data showed that the proton of OH enolate group observed in the spectrum of the free H<sub>2</sub>mel is not observed in the complexes spectra due to Hmel<sup>-</sup> is involved in a strong intra molecular hydrogen bond to the enolate oxygen comes in consistence with the data previously obtained from the infrared spectrum. The results of this investigation shore the proposed octahedral structure of the metal complexes and form a suitable molecular arrangement. The results obtained from DFT calculations point out that the complexes found in the octahedral geometrical structure which is very good with the experimental data. Complex (F) showed a higher cytotoxicity activity against MCF-7 human breast cancer cells cancer cell and HepG2 human liver carcinoma cell than free H<sub>2</sub>mel and Phen pointing out boosted antitumor activity upon coordination. This could be a step forward to apply this complex clinically on experimental models as therapeutic agents for liver and breast cancer.

## Conflicts of interest

“There are no conflicts to declare”.

## References

1. Roat-Malone, R.M., *Bioinorganic Chemistry: A short Course*. John Wiley and Sons, Inc, 2002. <https://doi.org/10.1002/0471265330.fmatter>
2. Crichton, R.R., *Biological Inorganic Chemistry an Introduction*, Elsevier, 2008. <https://doi.org/10.1016/C2016-0-01804-1>
3. Prakash O., Kumar R., Tyagi P. and Kuhad R.C., Organoiodine(III) mediated synthesis of 3,9-diaryl- and 3,9-difuryl-bis-1,2,4-triazolo[4,3-a][4,3-c] pyrimidines as antibacterial agents. *Eur. J. Med. Chem.*, 42, 868-872 (2007). <https://doi.org/10.1016/j.ejmech.2006.11.019>
4. Mohamed G.G., Synthesis, characterization and biological activity of bis(phenylimine) Schiff base ligands and their metal complexes. *Spectrochim. Acta A*, 64, 188-195 (2006). <https://doi.org/10.1016/j.saa.2005.05.044>
5. Mohamed G.G. and El-Gamel N.E.A., Preparation and spectroscopic characterisation of metal complexes of piroxicam. *Vib. Spectrosc.*, 36, 97-104 (2004). <https://doi.org/10.1016/j.vibspec.2004.04.004>
6. Sanatkar T.H., Hadadzadeh H., Simpson J. and Jannesari Z., The meloxicam complexes of Co(II) and Zn(II): Synthesis, crystal structures, photo cleavage and in vitro DNA-binding. *J. Mol. Struct.*, 1049, 336-344 (2013). <https://doi.org/10.1016/j.molstruc.2013.06.070>

7. Yuan Y., Chen X. and Zhong D., Determination of meloxicam in human plasma by liquid chromatography–tandem mass spectrometry following transdermal administration. *J. Chromatogr. B*, 852, 650-654 (2007). <https://doi.org/10.1016/j.jchromb.2007.01.036>
8. Defazio S. and Cini R., Synthesis, X-ray structural characterization and solution studies of metal complexes containing the anti-inflammatory drugs meloxicam and tenoxicam. *Polyhedron*, 22, 1355-1366 (2003). [https://doi.org/10.1016/S0277-5387\(03\)00112-8](https://doi.org/10.1016/S0277-5387(03)00112-8)
9. Mohamed G.G. and El-Gamel N.E.A., Synthesis, investigation and spectroscopic characterization of piroxicam ternary complexes of Fe(II), Fe(III), Co(II), Ni(II), Cu(II) and Zn(II) with glycine and dl-phenylalanine. *Spectrochim. Acta A*, 60, 3141-3154 (2004). <https://doi.org/10.1016/j.saa.2004.01.035>
10. Sadeek S.A. and Abd El-Hamid S.M., Preparation, characterization and cytotoxicity studies of some transition metal complexes with ofloxacin and 1,10-phenanthroline mixed ligand. *J. Mol. Struct.*, 1122, 175-185 (2016). <https://doi.org/10.1016/j.molstruc.2016.05.101>
11. Beecher D.J. and Wong A.C., Identification of hemolysin BL-producing *Bacillus cereus* isolates by a discontinuous hemolytic pattern in blood agar. *Appl. Environ. Microbiol.*, 60, 1646-1651 (1994). <https://doi.org/10.1128/AEM.60.5.1646-1651.1994>
12. Fallik E., Klein J., Grinberg S., Lomaniee E., Lurie S. and Lalazar A., Effect of Postharvest Heat Treatment of Tomatoes on Fruit Ripening and Decay Caused by *Botrytis cinerea*. *Plant Dis.*, 77, 985-988 (1993). <https://doi.org/10.1094/PD-77-0985>
13. Saotome K., Morita H. and Umeda M., Cytotoxicity test with simplified crystal violet staining method using microtitre plates and its application to injection drugs. *Toxicol. In Vitro.*, 3, 317-321 (1989). [http://dx.doi.org/10.1016/0887-2333\(89\)90039-8](http://dx.doi.org/10.1016/0887-2333(89)90039-8)
14. Seco J.M., Quiros M. and Garmendia M.J., Synthesis, X-ray crystal structure and spectroscopic, magnetic and EPR studies of copper(II) dimers with methoxy-di-(2-pyridyl)methoxide as bridging ligand. *Polyhedron*, 19, 1005-1013 (2000). [https://doi.org/10.1016/S0277-5387\(00\)00356-9](https://doi.org/10.1016/S0277-5387(00)00356-9)
15. Elshafie H.S., Sadeek S.A., Zordok W.A. and Mohamed A.A., Meloxicam and Study of Their Antimicrobial Effects against Phyto- and Human Pathogens. *molecules*, 26, 1480 (2021). <https://doi.org/10.3390/molecules26051480>
16. Li Y., Chai Y., Yuan R. and Liang W., Synthesis and application of a new copper(II) complex containing oflx and leof. *Russ. J. Inorg. Chem.*, 53, 704-706 (2008). <https://doi.org/10.1134/S0036023608050070>
17. Chawla S.K., Arora M., Nättinen K., Rissanen K. and Yakhmi J.V., Syntheses and crystal structures of three novel Cu(II) coordination polymers of different dimensionality constructed from Cu(II) carboxylates (carboxylate = malonate (mal), 2 acetate (ac), fumarate (fum)) and conformationally flexible 1,4-bis(imidazole-1-yl-methylene)benzene (IX). *Polyhedron*, 23, 3007-3019 (2004). <https://doi.org/10.1016/j.poly.2004.08.025>
18. Kose D.A., Kaya A. and Necefoglu H., Synthesis and characterization of bis(N,N-diethylnicotinamide) m-hydroxybenzoate complexes of Co(II), Ni(H), Cu(II), and Zn(II). *Russ. J. Coord. Chem.*, 33, 422-427 (2007). <https://doi.org/10.1134/S1070328407060073>
19. Sadeek S.A., Refat M.S. and Hashem H.A., Complexation and thermogravimetric investigation on tin(II) and tin(IV) with norfloxacin as antibacterial agent. *J. Coord. Chem.*, 59, 759-775 (2006). <https://doi.org/10.1080/00958970500404534>
20. Mondal N., Dey D.K., Mitra S. and Abdul Malik K.M., Synthesis and structural characterization of mixed ligand η<sup>1</sup>-2-hydroxyacetophenone complexes of cobalt(III). *Polyhedron*, 19, 2707-2711 (2000). [https://doi.org/10.1016/S0277-5387\(00\)00584-2](https://doi.org/10.1016/S0277-5387(00)00584-2)
21. Mohamed G.G. and Abd El-Wahab Z.H., Salisaldehyde-2-aminobenzimidazole schiff base complexes of Fe(III), Co(II), Ni(II), Cu(II), Zn(II) and Cd(II). *J. Therm. Anal.*, 73, 347-359 (2003). <https://doi.org/10.1023/A:1025126801265>
22. Masoud M.S. and Zaki Z.M., Synthesis and characterization of 5-(arylo)thiobarbituric acids and their complexes. *Trans. Met. Chem.*, 13, 321-327 (1988). <https://doi.org/10.1007/BF01225119>
23. Lever A.B.P., *Inorganic electronic spectroscopy*, 2, 480 (1984). <https://doi.org/10.1002/bbpc.19850890122>
24. Abd El-Hamid S.M., Sadeek S.A., Zordok W.A. and El-Shwiniy W.H., Synthesis, spectroscopic studies, DFT calculations, cytotoxicity and antimicrobial activity of some metal complexes with ofloxacin and 2,2'-bipyridine. *J. Mol. Struct.*, 1176, 422-433 (2019). <https://doi.org/10.1016/j.molstruc.2018.08.082>
25. Sadeek S.A., El-Attar M.S. and Abd El-Hamid S.M., Complexes and Chelates of Some Bivalent and Trivalent Metals with Ciprofloxacin Schiff Base. *Synth. React. Inorg. Met. Org. Chem.*, 45, 1412-1426

- (2015). <http://dx.doi.org/10.1080/15533174.2013.862686>
26. Khedr A.M. and Draz D.F., Synthesis, spectroscopic, and thermal analyses of trinuclear Mn(II), Co(II), Ni(II), and Zn(II) complexes with some sulfa derivatives. *J. Coord. Chem.*, 63, 1418-1429 (2010). <https://doi.org/10.1080/00958971003774241>
27. Abd El-Hamid S.M., Sadeek S.A., Zordok W.A. and Rashid N.G., Spectroscopic properties, molecular structure, anticancer and antimicrobial evaluation of some new moxifloxacin metal complexes in the presence of 1,10-phenanthroline. *Bull. Chem. Soc. Ethiop.* 34, 295-312 (2020). <https://dx.doi.org/10.4314/bcse.v34i2.8>
28. Chin L.M., Shun L.T. and Sartorelli A.C., 1 Chemical and Biological Properties of Cytotoxic  $\alpha$ -(N)-Heterocyclic Carboxaldehyde Thiosemicarbazones. *Progress in Med. Chem.*, 32, 1-35 (1995). [https://doi.org/10.1016/S0079-6468\(08\)70451-X](https://doi.org/10.1016/S0079-6468(08)70451-X)
29. Odunola O.A., Adeoye I.O. and Woods J.A.O., Synthesis and structural features of copper(II) complexes of benzoic acid and methyl substituted benzoic acid hydrazides and X-ray structure of  $\text{Cu}[\text{C}_6\text{H}_5\text{CONHNH}_2]_2(\text{NO}_3)_2$ . *Synth. React. Inorg. Met. Org. Chem.*, 32, 801-817 (2002). <https://doi.org/10.1081/SIM-120004447>
30. Frisch M.J., et. al., Gaussian 98, Revision A. 6, Inc., Pittsburgh PA, 1998.
31. Stevens W.J., Krauss M., Bosch H. and Jasien P.G., Relativistic compact effective potentials and efficient, shared-exponent basis-sets for the 3rd-row, 4th-row, and 5th-row atoms. *Can. J. Chem.*, 70, 612-630 (1992). <https://doi.org/10.1139/v92-085>
32. Change R., Physical Chemistry for Chemical and Biological Sciences, University Science Books, USA, 2000. <https://doi.org/10.1007/s0089700037a>
33. Tamasi G., Serinelli F., Consumi M., Magnani A., Casolaro M. and Cini R., Release studies from smart hydrogels as carriers for piroxicam and copper(II)-oxicam complexes as anti-inflammatory and anti-cancer drugs. X-ray structures of new copper(II)-piroxicam and -isoxicam complex molecules. *J. Inorg. Biochem.*, 102, 1862-1873 (2008). <https://doi.org/10.1016/j.jinorgbio.2008.06.009>
34. Abu-Eittah R.H. and Zordok W.A., A molecular orbital treatment of piroxicam and its  $\text{M}^{2+}$ -complexes: The change of the drug configuration in a time of bond formation. *J. Mol. Struct.: THEOCHEM.*, 951, 14-20 (2010). <https://doi.org/10.1016/j.theochem.2010.03.034>
35. Cini R., Tamasi G., Defazio S. and Hursthouse M.B., Unusual coordinating behavior by three non-steroidal anti-inflammatory drugs from the oxicam family towards copper(II). Synthesis, X-ray structure for copper(II)-isoxicam, -meloxicam and -cinnoxicam-derivative complexes, and cytotoxic activity for a copper(II)-piroxicam complex. *J. Inorg. Biochem.*, 101, 1140-1152 (2007). <https://doi.org/10.1016/j.jinorgbio.2007.04.015>
36. Pathak C., Gangwar M.K. and Ghosh P., Homodinuclear  $[\text{Fe}(\text{III})-\text{Fe}(\text{III})]$  and  $[\text{Zn}(\text{II})-\text{Zn}(\text{II})]$  complexes of a binucleating  $[\text{N}_4\text{O}_3]$  symmetrical ligand with purple acid phosphatase (PAP) and zinc phosphoesterase like activity. *Polyhedron*, 145, 88-100 (2018). <https://doi.org/10.1016/j.poly.2018.01.029>
37. Ciofini I., Laine P.P., Bedioui F. and Admo C., Photoinduced Intramolecular Electron Transfer in Ruthenium and Osmium Polyads: Insights from Theory. *J. Am. Chem. Soc.*, 126, 10763-10777 (2004). <https://doi.org/10.1021/ja0482278>
38. Ciofini I., Daul C. and Adamo C.J., Phototriggered Linkage Isomerization in Ruthenium-Dimethylsulfoxide Complexes: Insights from Theory. *J. Phys. Chem. A*, 107, 11182-11190 (2003). <https://doi.org/10.1021/jp0307607>
39. Casida M.E., In Recent Advances in Density Functional Methods, part 1; Chong D.P., Eds.; World Scientific: Singapore, 1995. [https://doi.org/10.1142/9789812830586\\_0005](https://doi.org/10.1142/9789812830586_0005)
40. Bauernschmitt R. and Ahlrichs R., Treatment of electronic excitations within the adiabatic approximation of time dependent density functional theory. *Chem. Phys. Lett.*, 256, 454-464 (1996). [https://doi.org/10.1016/0009-2614\(96\)00440-X](https://doi.org/10.1016/0009-2614(96)00440-X)

دراسات طيفية توصيفية وحرارية و نظرية الدوال الوظيفية والبيولوجية لبعض مترابطات المعادن الإنتقالية مع خليط من الميلوكسيكام و 1،10 فينانثرولين

صديق عطية صديق<sup>1</sup> و أميرة أحمد محمد<sup>2</sup> و وائل عبد الله زردق<sup>3</sup> و هانم محمد عوض<sup>4</sup> و شريف محمد عبد الحميد<sup>5</sup>

قسم الكيمياء- كلية العلوم- جامعة الزقازيق- الزقازيق- مصر<sup>1</sup>

قسم العلوم الأساسية – معهد الزقازيق العالى للهندسة والتكنولوجيا- الزقازيق- مصر<sup>2</sup>

قسم الكيمياء- الكلية الجامعية بالفتحة- جامعة أم القرى- السعودية<sup>3</sup>

قسم دباغة المواد وتكنولوجيا الجلود ، مركز التميز ، المركز القومي للبحوث ، القاهرة ، مصر<sup>4</sup>

قسم العلوم الأساسية – معهد المستقبل العالى للهندسة والتكنولوجيا- المنصورة- مصر<sup>5</sup>

تم تحضير سلسلة من المترابطات النشطة بيولوجيا باستخدام الميلوكسيكام و 1،10- فينانثرولين أحادى ماء التبلور. تم توصيف جميع المترابطات بواسطة الأشعة تحت الحمراء ، الإمتصاص الإلكتروني ، أطيف الرنين النووي المغناطيسى البروتوني ، و التحليل العنصرى ، العزم المغناطيسى ، التوصيل الكهربى والقياسات الحرارية. أوضحت النتائج الطيفية و التحليلية أن الميلوكسيكام يعمل كقاعدة أحادية ثنائية العطاء من خلال أكسجين الأמיד والنيتروجين لمجموعتي الثايزول ، بينما يرتبط الفيانثرولين من خلال ذرتي النيتروجين لتكوين مترابطات ثمانية الأوجه الغير متماثلة. تمت دراسة الأشكال الهندسية لليجندات والمترابطات باستخدام نظرية الدوال الوظيفية لتحديد خصائص المواد التي درستها طريقة الدوال الوظيفية الهجينة B3LYP. جميع المترابطات التى تم دراستها تم حساب قيم  $\eta$  لجميع المترابطات حيث وجد انها تتراوح من 0.053 لمركب Fe(III) إلى 0.089 لمركب Zn(II) وكذلك قيم  $\sigma$  وتتراوح من 11.236 إلى 18.868 eV ، بينما  $\sigma$  و  $\eta$  للميلوكسيكام هي 0.14 و 7.14 eV ، على التوالي. تم اختبار النشاط المضاد للبكتيريا لليجندات والمترابطات المعدنية وأظهرت البيانات أن هذه المترابطات ذو أهمية ضد بعض الأنواع البكتيرية مقارنة بالميلوكسيكام.